Available online at www.sciencedirect.com
SCIENCE DIRECT®
Advances in Space Research 34 (2004) 451–455
ADVANCES IN SPACE RESEARCH (a COSPAR publication)
www.elsevier.com/locate/asr

Use of RHESSI observations to determine the origin and fate of non-thermal flare electrons

Marcos E. Machado [a,*], Cristina H. Mandrini [b]

[a] Comisión National de Actividades Espaciales, Paseo Colón 751, C1063ACH Buenos Aires, Argentina
[b] Instituto de Astronomía y Física del Espacio, IAFE, CC. 67 Suc. 28, 1428 Buenos Aires, Argentina

Received 13 December 2002; received in revised form 13 March 2003; accepted 11 January 2004

Abstract

Most analyses of the characteristics of hard X-ray emission from solar flares have relied on observations of the spectral, temporal and spatial intensity distribution obtained by different instruments and, in the majority of cases, different events. The Reuven Ramaty High Energy Spectroscopic Imager gives us the possibility of combining all three fundamental parameters in a single set of observations from the same instrument. In this paper, we describe a method to compute the distribution of hard X-ray emission in flare loops, which can be used to determine the characteristics of electron energization, transport and thermalization during short lived impulsive peaks.

Keywords: Solar flares; Hard X-rays; Particle acceleration

1. Introduction

It is well known that the hard X-ray (HXR) emission from solar flares is caused by the energization of electrons in the energy release region or regions. We have also known for a long time that the energy contained in these particles represents a major fraction of the total flare energy. Over the years we have also recognized the following aspects related to the HXR emission: (a) Typically double footpoint structures are observed in hard X-rays, although single coronal sources and multiple structures are also seen. (b) Although power law spectra are omnipresent during the early stages of the impulsive phase, a characteristic of non-thermal emission, the HXR spectra also show evidence of a superhot thermal component with a temperature of a few times 10^7 K (Lin et al., 1981). (c) Any temporal modulation observed in the recorded HXR emission must be, in some form, related to a modulation in the energy release process (Aschwanden et al., 1998; Brown et al., 1998; de Jager and de Jonge, 1978; Machado et al., 1993; van Beek et al., 1974).

Here we present a preliminary set of calculations of the distribution of HXR emission in a flare loop, based on the method developed for the Hard X-ray Imaging Spectrometer (HXIS that flew on board the Solar Maximum Mission) data analysis by Machado et al. (1985). The calculations are performed under the following assumptions: (a) The accelerated electron spectrum follows a power-law distribution with energy (E), $F_0(E) = AE^{-\delta}$. (b) The accelerated electrons travel parallel to field lines (no scattering). (c) Coulomb collisions are the only loss mechanism. (d) The initial density and temperature of the loop are uniform along its length. (e) At the feet of the loop, which is of constant cross-section and symmetrical, we introduce a dense pseudo-chromosphere, where electrons are effectively stopped.

Along the loop and the chromosphere, the collisional energy losses lead to an energy degradation or stopping of the beam electrons, given by

$$F(E) = F_0(E_0)\,\mathrm{d}E_0/\mathrm{d}E = F_0(E(1+2KN/E^2)^{1/2})/(1+2KN/E^2)^{1/2}, \quad (1)$$

* Corresponding author. Tel.: +54-11-4331-5283; fax: +54-11-4331-3446.
E-mail address: machado@conae.gov.ar (M.E. Machado).

0273-1177/$30 © 2004 COSPAR. Published by Elsevier Ltd. All rights reserved.
doi:10.1016/j.asr.2004.01.007

where N (cm^{-2}) $= n_0 \Delta z$ is the column depth at Δz (cm) from the acceleration site, n_0 is the initial density, E_0 is the cutoff energy, and $K = 2\pi e^4 \Lambda$, with e the electron charge and Λ the Coulomb logarithm.

The non-thermal HXR emission per unit length, from $N = 0$ cm^{-2}, to a column depth N is given by (see Brown and McClymont, 1975; Machado et al., 1985, for details),

$$(\mathrm{d}I/\mathrm{d}z)_{n-t} = CAn(N)\epsilon^{-\delta-1}(B(\delta, 1/2)/\delta)H(\beta, \delta), \qquad (2)$$

where C is defined in Brown and McClymont (1975), $n(N) = n_0$ is constant along the loop, $H(\beta, \delta)$ is an integral function, with $\beta = KN/\epsilon^2$, which gives information on the thick target fraction of the HXR yield at photon energy ϵ, as a function of position (Brown and McClymont, 1975).

We also compute, in a self-consistent manner, the energy deposition of the electrons in the beam along the loop (z-direction), and obtain an effective heating rate that leads to an equilibrium loop temperature (T) by equating the beam energy input to saturated conductive losses, assuming a given loop cross-section. This is given by:

$$(3/2)n_0 k(\mathrm{d}T/\mathrm{d}t) = P(\Delta N, t) - Q_{\mathrm{sat}}(t), \qquad (3)$$

where P is the beam power, k is the Boltzmann constant, Q_{sat} is the saturated heat flux (Duijveman et al., 1982) and ΔN denotes the column density of the heated region. This equation is valid as long as the heating timescale is shorter than the hydrodynamic response time ($\tau_{\mathrm{h}} = \Delta z/v_{\mathrm{s}}$, where v_{s} is the sound speed). Therefore, our calculations are particularly relevant to the study of short duration spikes or bursts observed in the Compton Gamma Ray observatory (CGRO) (Fishman et al., 1989) flare data as described in e.g. Machado et al. (1993) and Aschwanden et al. (1998).

2. Results of the calculations

In Fig. 1 we show the results of a set of calculations. They correspond to what can be considered a small event with $P = 1.0 \times 10^{28}$ erg s^{-1}, occurring in a 10,000 km

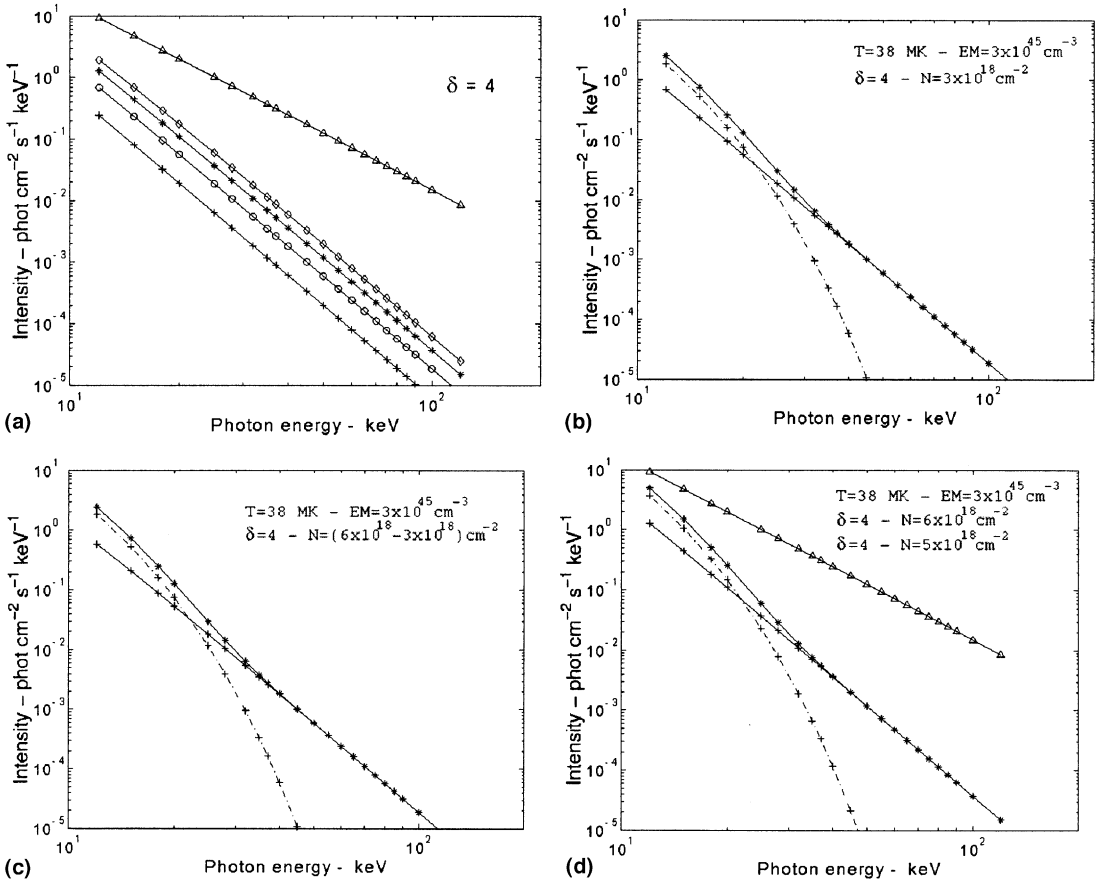

Fig. 1. (a) Total non-thermal HXR yield (from $N = 0$) at different column densities, N (cm^{-2}), from bottom to top $N = 1.0 \times 10^{18}$ cm^{-2} (crosses), $N = 3.0 \times 10^{18}$ cm^{-2} (circles), $N = 6.0 \times 10^{18}$ cm^{-2} (asterisks), $N = 1.0 \times 10^{19}$ cm^{-2} (diamonds), $N = 5.0 \times 10^{22}$ cm^{-2} (triangles). Note the hardening of the highest spectrum, that corresponds to emission from the chromospheric footpoint. (b) Total HXR yield from injection up to $N = 3.0 \times 10^{18}$ cm^{-2} (continuous line and crosses), the thermal contribution from the 3.8×10^7 K plasma (dash-dotted line and crosses) for an emission measure of EM $= 10^{45}$ cm^{-3}, and the summation of both contributions (continuous line and asterisks). (c) Same as (b), for $3.0 \times 10^{18} \leqslant N \leqslant 6.0 \times 10^{18}$ cm^{-2} (same convention as in (b)). (d) Total HXR yield of the looptop ($0 \leqslant N \leqslant 6.0 \times 10^{18}$ cm^{-2}), including the hot plasma thermal contribution (same convention as in (b)). Added the chromospheric footpoint contribution, $N = 5.0 \times 10^{22}$ cm^{-2} (continuous line and diamonds).

loop with a cross-section, 1.0×10^{17} cm^2). Fig. 1(a) shows a set of non-thermal spectra as function of column depth, these are computed for an injection spectral index $\delta = 4$. The characteristic hardening of the spectrum, comparing the thin-target corona with the large N thick-target chromosphere is clearly seen. In Fig. 1(b) we depict the non-thermal spectrum obtained from $0 \leqslant N \leqslant 3.0 \times 10^{18}$ cm^{-2}, which would correspond to the first 3000 km of the loop if its density had been 10^{10} cm^{-3}. Since our thermal balance calculations predict that the loop could be heated to $\approx 3.8 \times 10^7$ K, we also show the thermal contribution due to this hot component and the sum of both non-thermal and thermal spectra. Similar calculations for the subsequent 3.0×10^{18} cm^{-2} along the flaring loop, which are obtained by subtracting the total yield from $0 \leqslant N \leqslant 3.0 \times 10^{18}$ cm^{-2} to the one calculated for $0 \leqslant N \leqslant 6.0 \times 10^{18}$ cm^{-2} can be seen in Fig. 1(c). Finally, Fig. 1(d) depicts the spectra of the loop top from $0 \leqslant N \leqslant 6.0 \times 10^{18}$ cm^{-2}, and the chromospheric footpoint component, where we observe the clear predominance of the footpoint component in the total HXR yield above 20 keV, as RHESSI observations of, e.g., a small event observed on February 20, 2002, show (note however that we have not considered the contribution of the lower temperature soft X-ray emitting plasma, which may be significant up to around 20 keV).

In Fig. 2 we show the result of another test run, where we have assumed that the energy release occurred solely in a thin loop (cross-section 1.0×10^{16} cm^2) with strong heating up to a temperature of 1.7×10^8 K, leading to a predominance of the thermal contribution. To date, as pointed out by one of the referees, neither RHESSI or other space-borne instruments with lower spectral and spatial resolution have observed such spectra. However, since strong heating is indeed predicted by our calculations, as well as other models, we show the results of this test run as an example of predicted spectra that could be compared with observations.

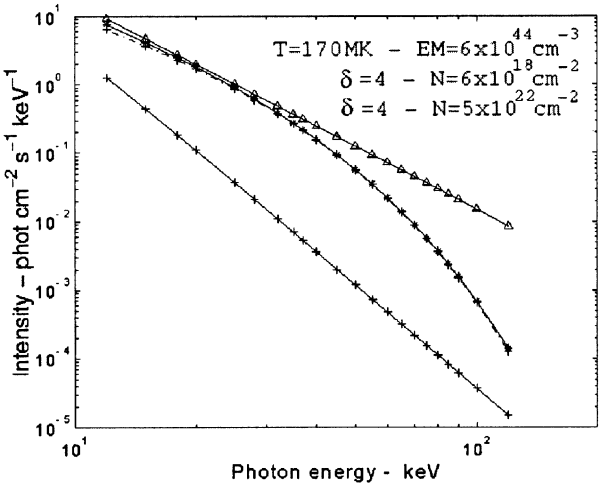

Fig. 2. HXR spectra of the looptop and footpoint (non-thermal component, same parameters as in Fig. 1(d), shown with continuous line and crosses), a hypothetical hot (1.7×10^8 K) thermal component with an EM $= 6.0 \times 10^{44}$ cm^{-3} (dash-dotted line and crosses) and their summation (continuous line and asterisks). See text for details.

3. Discussion

The calculations we have just described can be used for a straightforward and quick analysis of RHESSI (Lin et al., 1998) data on various types of events, with particular emphasis on those showing fast temporal structures. As we already mentioned, any modulation observed in the recorded HXR emission must be, in some form, related to a modulation in the energy release process. This was first recognized by van Beek et al. (1974) and de Jager and de Jonge (1978). From their analysis of the TD1-A spacecraft data, they indicated that HXR bursts could in general be decomposed into a number of short-lived spikes of duration ranging from a few seconds to a few tens of seconds. They called these spikes "elementary flare bursts" (EFBs), and suggested that represented the fundamental timescale of flare energy release. HXR emission recorded by the Burst and Transient Source Experiment (BATSE, Fishman et al., 1989) aboard CGRO, produced a wealth of data on high temporal resolution HXR burst observations of unprecedented quality. Machado et al. (1993), discussed some of its early results and demonstrated the capability of BATSE large area detector (LAD) modules to observe rapid fluctuations in their 64 ms resolution 4-channel spectrum mode. The feature that we want to stress is that HXR bursts show fine scale temporal structures with FWHM ranging between 200 and 700 ms. In a study of 647 events, Aschwanden et al. (1998), found that the shortest timescales detected in the strong flares range are from 0.1 to 0.4 s, while the most common short timescale observed in all flares is ≈ 0.5 s. As we know, the Bremsstrahlung emission process that leads to the production of HXR photons is well understood, prompt and optically thin. Therefore, it provides direct information on the particle energization process, free of model assumptions, unlike the case with most radio wave observations. However, unless the HXR observations have sufficient temporal and spectral resolution, the characteristics of the emission are inextricably coupled to transport processes and their associated effects (Emslie, 1983). In a series of papers, Aschwanden and collaborators (Aschwanden and Schwartz, 1995; Aschwanden et al., 1995, 1996a,b) have used medimum energy resolution (MER) BATSE data, together with Yohkoh soft X-ray images, to investigate the characteristics of short duration spikes and longer scale temporal fluctuations. In the case of the short duration spikes, they found that in many cases the softer

(25–50 keV) emission is delayed with respect to the higher energy emission (50–100 keV and above), by several tens of milliseconds. This is in agreement with the delays expected from time-of-flight differences, along a $\approx 10^4$ km flare loop, between electrons of similar energies producing the HXR emission by a thick target process. Although this is a general result regarding fast fluctuations, Aschwanden and collaborators also found many examples in which gradual HXR modulations show opposite delays, namely that the harder X-ray photon emission is considerably delayed with respect to the lower energies, by several (2–6) seconds. This type of delay can be explained by a trap-plus-precipitation model, where the HXR producing electrons are temporarily trapped in the flare loops before precipitating to the chromospheric footpoints. Delays are caused by trapping time differences, in terms of collisional deflection, between the lower energy electrons, that leak out first, and the higher energy electrons.

In the vast majority of the cases studied so far, the slowly varying component of the bursts may constitute up to 90% of the total HXR yield. This poses a basic question regarding the importance of the observed fine temporal structures, since they may lose the significance attributed to them by Machado et al. (1993), who proposed that they were the signature of the most elementary process of particle energization in solar flares and gave them the name of energy release fragments (ERFs). Clearly, the results of Aschwanden and collaborators are quite robust, since in many cases the slow component shows the characteristics of a trap-plus-precipitation environment. In such scenario, the bulk of the HXR emission is emitted at the footpoints after the high energy electrons, up to 90% of them according to the observed fluxes, are first trapped in the flaring loops. Although this is a logical interpretation, we should also bear in mind that the trapping plus precipitation just reflects the fate of the electrons after they are energized, rather than the detailed behavior of the primary energization process. Instead, the short timescale spikes give direct evidence of the result of particle energization at its source. This is shown by the observed energy dependent time delays, which indicate the absence of transport effects, other than those associated with electron time of flight differences from the acceleration site to the chromospheric footpoints. We thus contend that the fast spikes do show the signature of fragmentation in the flare energy release process. They represent those cases, out of the whole distribution, in which the particles precipitate directly to the footpoints in a classic thick target model fashion. The corresponding fraction is thus of the order of 10%, indicating that there is no preferred field-aligned acceleration in the flare loops, but rather an isotropic injection of the energetic particles.

Furthermore it is worthwhile mentioning that very recently, Masuda and Hudson (2002, unpublished, see SXT Weekly Science Nugget, 26-Jul-2002, http://solar.physics.montana.edu/nuggets/2002/index02.html) have found, in previously rarely used 0.5 s temporal resolution Yohkoh Hard X-ray Telescope images, that the footpoint morphology, when comparing 33–53 keV and 53–93 keV images in a large flare, seems to best correlate with a one second temporal displacement, with the highest energy images lagging in time. This type of delay is thus opposite to what can be expected from electron travel time arguments (which would not be as large in any case), and the measured delay is much shorter than those predicted by the particle trapping timescales reported by Aschwanden, but of same order of "typical" fast temporal fluctuations. The results (albeit very preliminary) may thus have important information on the particle injection profile as a function of time and energy or, in other words, the temporal evolution of the electron energization profile. We believe that RHESSI data, with its higher sensitivity and spectral resolution, will be ideal for this type of study. Using the method described above, we can obtain a self-consistent picture of the HXR emission along the flare loops and the chromosphere on the required timescales. One could in principle also detect, as shown in Fig. 2, the presence of any possible high temperature plasma component that may coexist with, or be part of, the energization process.

Acknowledgements

M.E.M. thank COSPAR and the UN Office for Outer Space Affairs, for the financial support that allowed him to attend the meeting.

References

Aschwanden, M.J., Schwartz, R.A. Accuracy, uncertainties and delay distribution of electron time-of-flight measurements in solar flares. Astrophys. J. 455, 699, 1995.

Aschwanden, M.J., Schwartz, R.A., Alt, D.M. Electron time of flight differences in solar flares. Astrophys. J. 447, 293, 1995.

Aschwanden, M.J., Wills, M.J., Hudson, H.S., Kosugi, T., Schwartz, R.A. Electron time-of-flight, distances and flare loop geometries compared from CGRO and Yohkoh observations. Astrophys. J. 468, 398, 1996a.

Aschwanden, M.J., Kosugi, T., Hudson, H.S., Wills, M.J., Schwartz, R.A. Electron time-of-flight measurements during the Masuda flare, 1992 January 13. Astrophys. J. 470, 1198, 1996b.

Aschwanden, M.J., Kliem, B., Schwarz, U., Kurths, J., Dennis, B.R., Schwartz, R.A. Wavelet analysis of solar flare hard X-rays. Astrophys. J. 505, 941, 1998.

Brown, J.C., McClymont, A.N. Oscillations of coronal electron traps inferred from hard X-ray data. Solar Phys. 41, 135, 1975.

Brown, J.C., Conway, A.J., Aschwanden, M.J. The electron injection function and energy-dependent delays in thick-target hard X-rays. Astrophys. J. 509, 911, 1998.

de Jager, C., de Jonge, G. Properties of elementary flare bursts. Solar Phys. 58, 127, 1978.

Duijveman, A., Hoyng, P., Machado, M.E. X-ray imaging of three flares during the impulsive phase. Solar Phys. 81, 137, 1982.

Emslie, A.G. Thick target Bremsstrahlung interpretation of short time-scale solar hard X-ray features. Astrophys. J. 271, 367, 1983.

Fishman, G.J., et al. The BATSE experiment on the Gamma Ray Observatory: Solar flare hard X-ray and gamma-ray capabilities, in: Proceedings of the GRO Observatory Science Workshop, pp. 2–39, 1989.

Lin, R.P., Schwartz, R.A., Pelling, R.M., Hurley, K.C. A new component of hard X-rays in solar flares. Astrophys. J. 251, L109, 1981.

Lin, R.P., et al. High-Energy Solar Spectroscopic Imager (HESSI) Small Explorer mission for the next (2000) solar maximum, in: Korendyke, C.M. (Ed.), Proceedings of the SPIE, vol. 3442, pp. 2–12, Missions to the Sun II, 1998.

Machado, M.E., Rovira, M.G., Sneibrun, C.V. Hard X-ray imaging evidence of nonthermal and thermal burst components. Solar Phys. 99, 189, 1985.

Machado, M.E., Ong, K.K., Emslie, A.G., Fishman, G.J., Meegan, C., Wilson, R., Paciesas, W.S. The fine scale temporal structure of hard X-ray bursts. Adv. Space Res. 13 (9), 175, 1993.

van Beek, H.F., de Feiter, L.D., de Jager, C. Hard X-ray observations of elementary flare bursts and their interpretation. Space Res. 14, 447, 1974.